Journal of Inorganic Biochemistry 106 (2012) 32–42

Contents lists available at SciVerse ScienceDirect

Journal of Inorganic Biochemistry

journal homepage: www.elsevier.com/locate/jinorgbio

Overcoming cisplatin resistance using gold(III) mimics: Anticancer activity of novel gold(III) polypyridyl complexes

Kamalakannan Palanichamy [a], Nair Sreejayan [b], Allyn C. Ontko [c,*]

[a] Department of Radiation Oncology, The Ohio State University Medical Center, Columbus, OH 43210, USA
[b] School of Pharmacy, Division of Pharmaceutical Sciences and Center for Cardiovascular Research and Alternative Medicine, University of Wyoming, Laramie, WY 82071, USA
[c] Department of Chemistry and Physics, Arkansas State University, P.O. Box 419, State University, AR 72467, USA

ARTICLE INFO

Article history:
Received 21 May 2010
Received in revised form 18 August 2011
Accepted 19 August 2011
Available online 12 September 2011

Keywords:
Gold(III)
Au(III)
Polypyridyl
Cellular uptake
DNA binding affinity
Anticancer

ABSTRACT

Gold(III) compounds have been recognized as anticancer agents due to their structural and electronic similarities with currently employed platinum(II) species. An added benefit to gold(III) agents is the ability to overcome cisplatin resistance. This work identified four gold(III) compounds, $[Au(Phen)Cl_2]PF_6$, $[Au(DPQ)Cl_2]PF_6$, $[Au(DPPZ)Cl_2]PF_6$, and $[Au(DPQC)Cl_2]PF_6$, (Phen = 1,10-phenanthroline, DPQ = dipyrido[3,2-d:2′,3′-f]quinoxaline, DPPZ = dipyrido[3,2-a:2′,3′-c] phenazine, DPQC = dipyrido[3,2-d:2′,3′-f] cyclohexyl quinoxaline) that exhibited anticancer activity in both cisplatin sensitive and cisplatin resistant ovarian cancer cells. Two of these compounds, $[Au(DPQ)Cl_2]PF_6$ (AQ) and $[Au(DPPZ)Cl_2]PF_6$ (AZ), displayed exceptional anticancer activity and were the focus of more intensive mechanistic study. At the molecular level, AQ and AZ formed DNA adducts, generated free radicals, and upregulated pro-apoptotic signaling molecules (p53, caspases, PARP, death effectors). Taken together, these two novel gold(III) polypyridyl complexes exhibit potent antitumor activity in cisplatin resistant cancer cells. These activities may be mediated, in part, by the activation of apoptotic signaling.

1. Introduction

Platinum-containing compounds such as cisplatin, carboplatin and oxaliplatin are widely used in the treatment of a variety of cancers. Newer, second generation platinum compounds like carbo- and oxali-platin were designed to improve efficacy particularly against cell lines that demonstrate second pass cisplatin resistance [1]. Tolerance to cisplatin-induced DNA damage has been suggested as a fundamental mechanism of drug resistance [2]. Cisplatin resistance is thought to occur primarily by cells resisting DNA platination leading to the exit at G2/M phase of cell cycle and inhibiting apoptosis [3]. In addition, drug-efflux in resistant cell lines has been shown to be greater than the influx due to the up-regulation of multi drug resistance (MDR) genes and the production of antiporters such as p-glycoprotein [3]. To circumvent the problem of drug-resistance in cisplatin-resistant cells, gold(III)-based complexes have been designed as a potential alternative to cisplatin [4–8]. Gold(III) complexes exhibit isoelectronic and isostructural features with platinum (II) and have similar uptake and DNA interference activity[8]. In addition, the higher charge of gold(III) compared to platinum(II) is an added advantage for binding with DNA [5, 9].

One recent active area of interest is the design and characterization of small complexes with polypyridyl and phenanthroline ligands for use as structural DNA probes or artificial nucleases [10–15]. Since transition metal complexes of polypyridyl ligands can bind to specific DNA sequences [16], one can hope to achieve selective binding of mutated or altered DNA sequence in cancer cells compared to non-transformed cells, thereby decreasing the unwanted toxicity due to chemotherapeutics. As drug efflux is believed to be an important contributing factor in cisplatin resistance, polypyridyl ligands, owing to their stronger DNA binding capacity, may decrease resistance via cellular efflux.

While many studies report that gold(III) complexes are emerging as potential anticancer targets [17–25], few detailed mechanistic studies exist. To this end, this work evaluates the cytotoxic activity, cellular uptake, intracellular signaling cascades and DNA binding affinity of gold(III) polypyridyl complexes in cisplatin-sensitive, cisplatin-resistant and multidrug resistant ovarian cancer cells.

2. Experimental

2.1. Materials and method

The gold polypyridyl complexes $[Au(Phen)Cl_2]PF_6$, $[Au(DPQ)Cl_2]PF_6$, $[Au(DPPZ)Cl_2]PF_6$, and $[Au(DPQC)Cl_2]PF_6$ (Phen = 1,10-phenanthroline, DPQ = dipyrido[3,2-d:2′,3′-f]quinoxaline, DPPZ = dipyrido

* Corresponding author. Tel.: +1 870 972 3472.
E-mail address: aontko@astate.edu (A.C. Ontko).

0162-0134/$ – see front matter © 2011 Elsevier Inc. All rights reserved.
doi:10.1016/j.jinorgbio.2011.08.013

[3,2-a:2′,3′-c] phenazine, DPQC = dipyrido[3,2-d:2′,3′-f] cyclohexyl quinoxaline) were synthesized using analytical grade reagents and HPLC quality solvents (Fig. 1). The synthesis of the ligands and complexes has been reported elsewhere [8]. Adherent human ovarian adenocarcinoma cells (A2780) used for cytotoxicity studies were obtained from The National Cancer Institute-Frederick Cancer DCI Tumor Repository. The cisplatin-sensitive A2780 cells were exposed to cisplatin to generate cisplatin resistant A2780CP70 (IC_{50} ~70 μM) cell line (generously donated by Dr. J. Christopher States, University of Louisville College of Medicine, Louisville, KY). The Hank's balanced salt solution, Dulbecco's-phosphate buffer saline, biological grade DMSO, and Triton X-100 were purchased from Sigma (St. Louis, MO). The RPMI-1640 medium (ATCC), penicillin, streptomycin, fetal bovine serum (FBS) and trypsin-EDTA were from Invitrogen Corporation (Carlsbad, CA). RPMI-1640 medium was supplemented with 5% heat inactivated FBS, penicillin and streptomycin. Multidrug-resistant cell line HTB-161 or OVCAR-3 cell line was obtained from American Type Culture Collection (Manassas, VA). This cell line is resistant to clinically relevant concentrations of adriamycin, melphalan and cisplatin. The HTB-161 cells were propagated in RPMI-1640 Medium containing 0.01 mg/ml bovine insulin and fetal bovine serum to a final concentration of 20%. Normal ovarian cancer cell line CRL-9096 from hamster also obtained from ATCC was grown in Iscove's modified Dulbecco's medium with 4 mM L-glutamine adjusted to contain 1.5 g/L sodium bicarbonate and supplemented with 0.1 mM hypoxanthine, 0.016 mM thymidine, 0.002 mM methotrexate and 10% FBS. These cells are deficient in dihydrofolate reductase and will die in the absence of hypoxanthine–thymidine. Methotrexate was added to the cell culture medium to prevent growth of revertant cells with a low resistance to the drug. Costar brand sterile, tissue culture treated 96-well black clear bottom plates were purchased from Corning (Corning, NY). The Live/Dead cell viability/cytotoxicity kit was purchased from Molecular Probes (Carlsbad, CA) and cell viability was assessed per manufacturer's protocol. The compounds were initially dissolved in DMSO, and further dilutions were made with complete medium. The final concentration of DMSO did not exceed 5% in any of the experiments and similar amounts of DMSO were added to control cells.

2.2. In-vitro cytotoxicity assay

All the cell lines were cultured in a humidified atmosphere of 5% CO_2/95% air, adhesion of cells (~50%) to the culture surface occurred within the first few hours after seeding. Rapid growth was observed thereafter following overnight incubation. The cells were allowed to reach about 70% confluence at which time the cells were washed with Hank's balanced salt solution and harvested using standard trypsin-EDTA method. The harvested cells were seeded in 96-well black clear bottom tissue culture plates and allowed to grow to about 90% confluence in supplemented growth medium. At this stage, the medium was aspirated and the cells were washed with Dulbecco's-phosphate buffered saline (D-PBS). Subsequently, the cells were incubated for 2 h in D-PBS solution containing varying concentrations of $NaAuCl_4 \cdot 2H_2O$, polypyridyl ligand, Au-ligand complex or the standard drug cisplatin in DMSO at the concentrations. Control wells containing similarly grown cells were treated with 5% DMSO. In some experiments cells were incubated with a 5% Triton-X100 as a positive control to assess cell death. All wells were treated with Live/Dead viability/cytotoxicity reagent and the dye concentration and incubation time optimized. After incubation for 2 h, 50 μL of Live cell reagent (1 μL calcein AM/1 mL of D-PBS) was added to wells and then incubated for further 2 h. Fluorescence was measured at excitation and emission wavelengths of 485 nm and 525 nm respectively using a 515 nm cut-off filter (Spectramax, Gemini Microplate Spectrofluorometer, Molecular Devices, Sunnyvale, CA). From the fluorescence intensities (obtained from the weighted average of twelve wells from quadruplet trials), the % inhibition was calculated. The inhibiting concentration (IC_{50}) was determined by plotting log (conc.) of test compounds vs. % inhibition. The % inhibition was also cross checked using a standard MTT (MTT = 3-(4,5-Dimethylthiazol-2-yl)-2,5-diphenyltetrazolium bromide) assay.

2.3. Drug treatment, total protein determination and sample preparation for inductively coupled plasma emission spectroscopy (ICP) analysis

The gold polypyridyl complexes $[Au(Phen)Cl_2]PF_6$, $[Au(DPQ)Cl_2]PF_6$, $[Au(DPPZ)Cl_2]PF_6$, and $[Au(DPQC)Cl_2]PF_6$ (10 μM) were added to cells during their growth-phase and incubated for 2 h. The cell monolayers were washed three times with cold PBS and harvested by trypsination and was completely eluted from the plate. The cell suspension was centrifuged at 1000 *g* for 5 min at 4 °C and the pellet was resuspended in D-PBS and was centrifuged at 1000 *g* for 5 min and was repeated once and the pellet was stored at −80 °C until use. The pellets were resuspended in mQ water to obtain a homogeneous cell suspension. Aliquots were removed and treated with radioimmunoprecipitation assay (RIPA) buffer sonicated and protein concentration of the lysate was determined by bicinchonic acid (BCA) assay. The remaining cell suspension was transferred into a glass tube containing 50% HNO_3 and was mineralized until complete drying at 120 °C. Dry gold containing materials were dissolved in 2 mL of 2% HNO_3 and the clear solution obtained was analyzed for total gold. Sonicated samples were assayed by BCA-method for their protein quantification.

2.4. Determination of reactive oxygen species (ROS)

The presence of intracellular reactive oxygen intermediates was measured based on the ability of cells to oxidize fluorogenic dyes to their corresponding fluorescent analogs. The non-ionic, nonpolar H_2DCF-DA crosses cell membranes and is hydrolyzed enzymatically by intracellular esterases to nonfluorescent DCFH. In the presence of

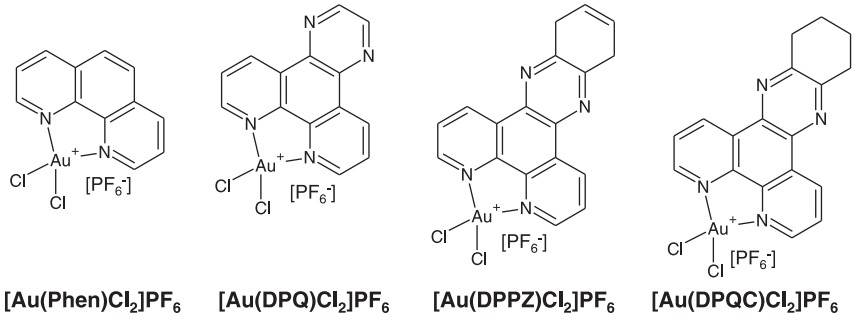

Fig. 1. Gold(III) polypyridyl complexes. Proposed structures of the gold(III) polypyridyl complexes.

ROS, DCFH is oxidized to highly fluorescent dichlorofluorescein (DCF). Medium was aspirated from the exponentially growing cultures of cells, the cells were washed with Krebs–Ringer–HEPES (KRH) buffer and then incubated with 5 μM of H_2DCFDA (Molecular Probes, Carlsbad, CA) for 30 min in 5% CO_2/95% air at 37 °C. After H_2DCFDA was removed, the cells were washed and incubated with KRH-buffer (with different concentrations of compounds) and the fluorescence of the cells from each well was measured at excitation and emission wavelengths of 485 nm and 530 nm respectively. Cells treated with H_2O_2 were used as positive control. Data points were taken every 5 min for 3 h and an optimum time of 2 h was identified. Fluorescence intensities (obtained from the weighted average of twelve wells from quadruplet trials), the ROS generated was calculated from the fluorescence intensities.

2.5. Circular dichroism (CD) measurements

CD spectra were recorded using a JASCO J-800 series spectropolarimeter in the UV region (220–300 nm). A quartz cell of path length 1 cm was used for the experiments. The instrument is controlled by JASCO's Spectra Manager software. In most cases, the optical densities of the solutions were maintained below 1.0 in the desired range. The signal to noise ratio was negligible above 220 nm, but below 220 nm the ratio was significant mainly because of the high absorbance of both Au(III) and DNA. All the measurements were carried out in physiological buffer at room temperature (32 °C), following equilibration for 12 h. Because calf thymus and plasmid DNA led to ambiguous results, short synthetic nucleotides were obtained from IDT Technologies (San Diego, CA) and annealed to form ds-DNA and used for the studies. The sense and anti-sense strands used were 5′-CTA TTG CAT AGC CTA TTG CAT AGC-3′ and 5′-GCT ATG CAA TAG GCT ATG CAA TAG-3′ respectively.

2.6. Restriction enzyme analysis

Plasmid DNA (pBR322, New England Biolabs, Ipswich, MA.) was incubated with gold polypyridyls (molar ratios ranging from 1:1, 1: 0.5, 1: 0.25, 0.25:1, and 0.5:1) in physiological buffer (50 mM phosphate, 4 mM NaCl, pH 7.4) for 24 h at 37 °C. DNA was precipitated with ethanol and resuspended in Tris-EDTA (TE) buffer, pH 8.0. The control DNA and gold polypyridyl-DNA complexes were digested with restriction endonuclease in appropriate buffers and were subjected to electrophoresis on 1% agarose gel for 3 h at 75 V in 1× TBE buffer. The gels were stained with ethidium bromide and photographed under UV lamp and the density of the linear versus open circular from of DNA was quantitated by densitometry (BioRad, Geldoc2000). The sequence specific binding ability of gold polypyridyls was inferred by assessing DNA breaks using various restriction endonucleases. DNA was incubated with compounds in physiological buffer and subjected to electrophoresis in 1% agarose gel following the digestion with *NaeI* and *DraI* of pUC19/pBR322 DNA covalently modified with gold polypyridyls. Two different restriction enzymes were used to estimate the specificity of the binding of gold polypyridyls. *DraI* recognizes the sequence "TTTAAA" (TA or AT) and cuts the phosphodiester bond between 3232, 3251 and 3943 bp. NaeI recognizes "GCCGGC" (CG or GC) and cuts between 403, 771, 931 and 1285 [26].

2.7. Electrophoresis, western blotting and intracellular signaling cascades

Effect of gold(III) polypyridyls on intracellular signaling cascades was assessed by western blot analysis. Briefly, cells were lysed in RIPA buffer (150 mM NaCl, 0.25% sodium deoxycholate, 1% NP-40, 1 mM EDTA and 50 mM Tris, pH 7.2) containing 2 mM sodium vanadate, 1 mM PMSF, l mM sodium fluoride, 1 μg/ml aprotinin, 1 μg/ml leupeptin, and 1 μM pepstatin and sonicated to reduce the sample viscosity. The lysate was centrifuged at 15,000 *g* for 15 min at 4 °C and the protein concentration in the supernatant was determined by the BCA-method. Equal amounts of total protein were boiled in Laemmli sample buffer. About 25 μg of whole cell extracts were resolved on a 7.5–10% polyacrylamide gel, and electrophoretically transferred to a nitrocellulose membrane. The membranes were incubated at for 1 h at room temperature in blocking buffer (5% w/v non-fat dry milk in tris buffered saline containing 0.1% Tween 20). Membranes were incubated in appropriate primary antibody mitogen activated protein kinase (Erk 1/2), phospho-Erk 1/2, stress activated protein kinase/c-jun n-terminal kinase (SAPK/JNK), phospho-SAPK/JNK, p38 (member of MAPK family-38KDA), phospho-p38, p53 (tumor suppressor protein-53 KDA), phospho-p53 (phosphorylated at ser15, ser20, ser37, ser46, ser303, ser392, PARP [poly(ADP)ribose polymerase]), cleaved-PARP, DNA fragmentation factor (DFF 45/35), cytochrome-c, caspase 3, cleaved caspase 3, BAD, BAK, BCL-XL, BAX, BAD, cdc2, phospho-cdc2 (Cell Signaling Technology Inc., Danvers, MA) and anti-α-actin (Sigma, St. Louis, MO) at 1:5000 dilutions in the blocking buffer for overnight at 4 °C followed by incubation with horseradish peroxidase-coupled secondary antibodies with appropriate specificity. Immunoreactive bands were visualized using enhanced chemiluminescence reagents (Cell Signaling Technology, Inc., Danvers, MA). Blots were then stripped and re-probed with other antibodies.

2.8. Assay for apoptosis

The apoptosis assay was performed using Annexin V-Biotin Apoptosis Detection Kit (Biovision Inc., CA). The cells were incubated with gold(III) polypyridyls and at the desired time point both the floating and adherent cells were collected, centrifuged and resuspended in 1× Binding buffer followed by incubation with Annexin V-Biotin and propidium iodide at room temperature for 5 min in the dark. The cells were subsequently washed once with 1× Binding buffer and fixed with 2% formaldehyde in PBS for 15 min and again washed with PBS and resuspended in PBS. The cell suspension was transferred to a glass slide and visualized under a fluorescence microscope using a dual filter set for FITC and rhodamine. Cells that have bound Annexin V-Biotin and stained with streptavidin-FITC will show green staining of the plasma membrane. Cells which have lost

Table 1
Cytotoxicity of gold(III) polypyridyls in A2780 and A2780-CP70 Cell lines.

Compounds	Concentration (μM) and% Growth Inhibition (±3) of A2780 cell line				IC_{50} (μM) A2780 (±2)	Concentration (μM) and% Growth Inhibition (±3) of A2780-CP70 cell line				IC_{50} (μM) A2780-CP70 (±2)
	0.05	0.5	5	50		0.05	0.5	5	50	
Cis Platin	8	21	28	47	55	5	9	13	34	100
$[Au(Phen)Cl_2]PF_6$	18	30	48	59	6	10	18	26	48	52
$[Au(DPQ)Cl_2]PF_6$	22	31	48	81	6	15	19	26	57	45
$[Au(DPPZ)Cl_2]PF_6$	19	22	28	52	45	20	29	41	68	6
$[Au(DPQC)Cl_2]PF_6$	16	29	48	67	6	15	20	27	63	40

membrane integrity will show red staining propidium iodide (PI) throughout the nucleus and a halo of green staining fluorescein isothiocyanate (FITC) on the cell surface (plasma membrane). We also assessed the formation of DNA fragments of oligonucleosomal size (180–200 bp), a hallmark of apoptosis using the Apoptotic DNA Ladder Kit (Roche Diagnostics) per manufacturer's protocol.

2.9. Data analysis

Data are expressed as means ± S.E.M. and statistically evaluated using Graph pad prism5. The analysis was conducted using two way repeated-measure analysis of variance (RM-ANOVA), and p values were calculated for interaction, row and column factor. Further, Bonferroni post-hoc test was done to determine the statistical significance.

3. Results and discussion

3.1. Cytotoxicity

The cytotoxic effect of gold(III) polypyridyls was tested at various concentrations ranging from 5 nM to 5 mM using standard MTT methods and live/dead cell assays. The results from these studies indicate that the IC_{50} values vary greatly among the compounds tested in both cisplatin-sensitive and -resistant cell lines (Table 1). Among the four compounds studied, the cytotoxicities of $[Au(DPQ)Cl_2]PF_6$ (81% growth Inhibition) and $[Au(DPPZ)Cl_2]PF_6$ (68% growth Inhibition) at 50 μM concentration were higher compared to $[Au(Phen)Cl_2]PF_6$ and $[Au(DPQC)Cl_2]PF_6$ in A2780 and A2780CP70 cells respectively. Representative data for cytotoxicity of gold(III) polypyridyls in cisplatin resistant A2780CP70, multidrug resistant HTB-161 and normal CRL-9096 cells are shown in Fig. 2. The cytotoxic effect of gold(III) polypyridyls was significantly higher than cisplatin in all the cancer cell lines tested. The% cell death induced by gold(III) complexes of DPQ and DPPZ at 50 μM were 57% and 68% respectively in A2780CP70 cell line, whereas the free ligands exhibited <10% cell death at equimolar concentrations. The enhanced cytotoxicity of the DPPZ complex may be attributed to a number of factors that will be described more fully in later sections. These include enhanced cellular uptake, enhanced generation of reactive oxygen species, enhanced DNA interaction due to the extended π array of the ligand, or changes in protein expression.

At all concentrations tested from 100 μM to 500 μM, the gold(III) polypyridyls inhibited cell growth to a greater extent than cisplatin with the DPPZ analog proving more effective than DPQ complex. Fig. 2, panel A shows the representative concentrations tested. Measured IC_{50} values of CP = 100 μM, AQ = 45 μM and AZ = 6 μM were obtained for the A2780DP70 line. The immunofluorescence images using live/dead cell reagent in A2780CP70 cell line are shown in Fig. 3. From the images it is evident that $[Au(DPQ)Cl_2]PF_6$ inhibited cell growth in a time dependent manner and the extent of inhibition was greater than that seen with cisplatin at similar concentrations at all time points. Interestingly, in contrast to cancer cells, in non-transformed normal CRL-9096 cells the cytotoxicity of gold(III) polypyridyls was significantly lower compared to that observed with cisplatin (Fig. 2 Panel-B). A tenfold higher concentration of gold(III) polypyridyls were required to observe similar cytotoxic effect as that of cisplatin in the non-cancerous cell lines. In healthy hamster ovarian cells, cisplatin was more toxic than the gold(III) polypyridyls tested at various concentrations (IC_{50}: CP = 35 μM, AQ = 70 μM and AZ = 110 μM). This observation is indicative of their reduced toxicity in normal cell lines and suggests that gold(III) polypyridyl complexes may be selectively targeting cancerous cells. However in the multidrug resistance cells, HTB-161, gold(III) polypyridyls exhibited greater cytotoxicity than cisplatin at all concentrations tested (Fig. 2 Panel-C). The HTB-161 cells represent an appropriate model system to study drug resistance in ovarian cancer and they exhibit androgen and estrogen receptors, demonstrate enhanced drug efflux, and contain a calcium channel blocker [27, 28]. The cytotoxicity exhibited by gold(III) polypyridyls in the HTB-161 cell line was similar (IC_{50}: CP = 65 μM, AQ = 50 μM and AZ = 42 μM) regardless of the ligands used, indicating that the nature of the ligand may not alter the cytotoxicity in these cells. These results suggest that normal cell and cancer cells differ in their sensitivity to gold(III) polypyridyl compounds.

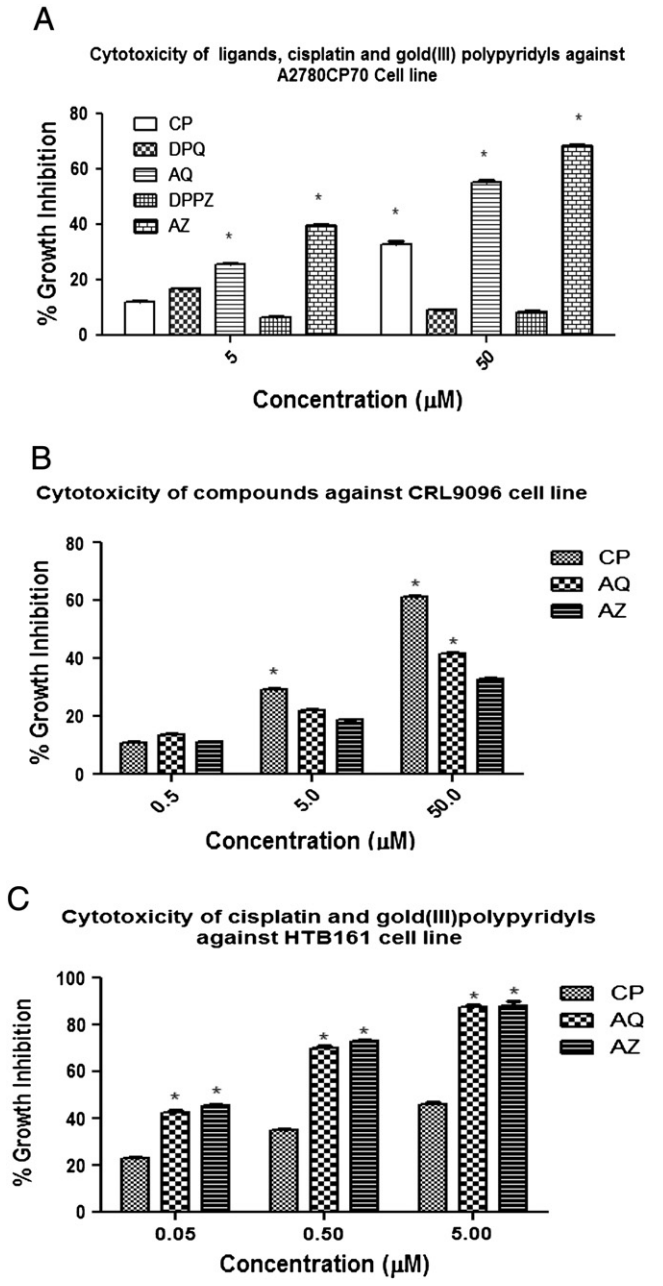

Fig. 2. Cytotoxicity of gold(III) polypyridyls. CP = Cisplatin, AQ = $[Au(DPQ)Cl_2]PF_6$, AZ = $[Au(DPPZ)Cl_2]PF_6$.The growth inhibition was computed as follows;

$$\%\ Growth\ Inhibition = \frac{A(con) - A(sample)}{A(con) \tilde{n} 100}$$

where A(con) = Absorbance of control well and A(sample) = Absorbance of sample well. Data analysis: Two way RM-ANOVA, p value < 0.0001 for interaction, row and column factor, Bonferroni post test: statistically significant ($p < 0.001$). Panel-A: Cytotoxicity in Cisplatin Resistant Ovarian A2780-CP70 Cell Line: Panel-B: Cytotoxicity in Normal Hamster Ovarian CRL9096 Cell Line: Panel-C: Cytotoxicity in Multidrug Resistant Ovarian HTB-161 Cell Line.

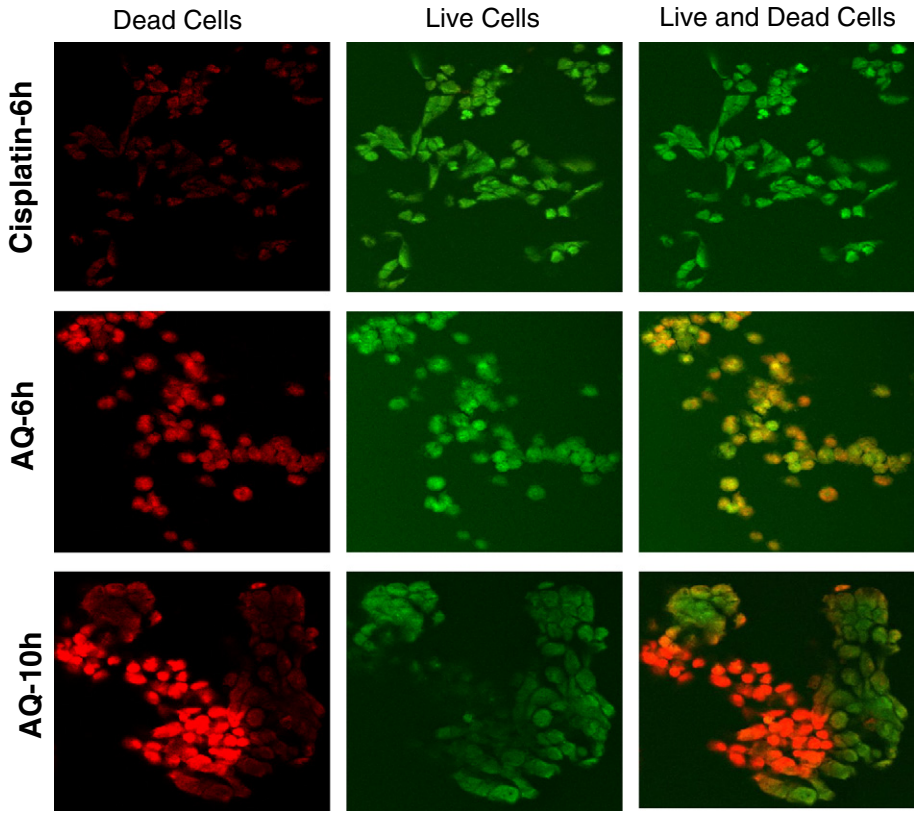

Fig. 3. IF images of $[Au(DPQ)_2Cl_2]PF_6$ (AQ) in A2780-CP70 cell line using live/dead cell reagent. After incubating the cells with $[Au(DPQ)_2Cl_2]PF_6$ (AQ) for 6 h, cells stained for dead cell reagent and after 10 h, the cell death was increased when compared to cisplatin the cell death was more with AQ treatment. The red and green fluorescence are the markers of dead and live cells respectively. The Live/Dead Viability/Cytotoxicity Assay Kit (Invitrogen-Molecular Probes) is a two-color fluorescence cell viability assay leads to a simultaneous determination of live and dead cells with two probes using calcein AM and ethidium homodimer (EthD-1). Live cells are distinguished by the presence of ubiquitous intracellular esterase activity, determined by the enzymatic conversion of the virtually nonfluorescent cell-permeant calcein AM to the intensely fluorescent calcein. The polyanionic dye calcein is well retained within live cells, producing an intense uniform green fluorescence in live cells (ex/em ~495 nm/~515 nm). EthD-1 enters cells with damaged membranes and undergoes a 40-fold enhancement of fluorescence upon binding to nucleic acids, thereby producing a bright red fluorescence in dead cells (ex/em ~495 nm/~635 nm). EthD-1 is excluded by the intact plasma membrane of live cells. The % Live/Dead cells after treatment were estimated by following the manufacturer's protocol. Triton-X100 was used as a positive control for cell death.

These results substantiate previous studies wherein gold(III) tetraarylporphyrins were shown to display preferential cytotoxicity toward cancer cells compared to normal cells [29]. In addition, the polypyridyl ligands in gold(III) complexes are known DNA binding agents and could enhance DNA interaction [16]. Enhanced cytotoxicity of gold(III) polypyridyls may be attributed to their increased affinity toward DNA due to their higher nuclear charge (+3) compared to platinum (+2). At all time points, gold(III) polypyridyls exhibited greater cytotoxicity than cisplatin.

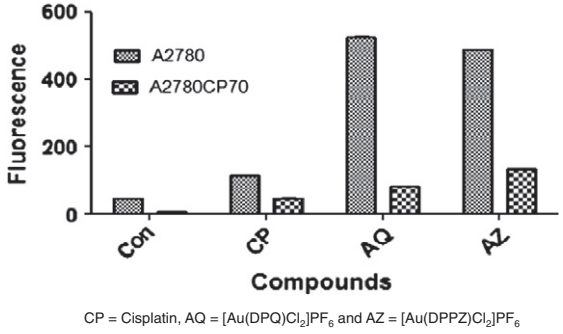

Fig. 4. Reactive oxygen species (ROS) generated after treating A2780 and A2780CP70 cell lines with gold(III) polypyridyls. Con = No treatment, CP = Cisplatin, AQ = $[Au(DPQ)Cl_2]PF_6$, AZ = $[Au(DPPZ)Cl_2]PF_6$. Data analysis: Two way RM-ANOVA, p value<0.0001 for interaction, row factor and column factor Bonferroni post test: statistically significant ($p<0.001$).

A major mechanism for drug resistance among metal-containing chemotherapeutic agents is the up regulation of drug resistance genes upon prolonged exposure of cells to drug [2, 30–32]. These genes encode for antiporter proteins, such as p-glycoprotein, that export compounds out of the cell as mechanism of cellular defense. As cellular efflux is a major cause of drug resistance, we assessed the cellular uptake of gold(III) polypyridyls using inductively coupled plasma emission spectroscopy (Table 2).

Table 2
Intracellular concentration of gold(III) polypyridyls in A2780 and A2780-CP70 Cell lines.

Sample	A2780			A2780-CP70		
	Protein (μg)	Au (ppb)	IC	Protein (μg)	Au (ppb)	IC
Control	45.21	0.4	0.88	58.10	6.1	10.50
$[Au(Phen)Cl_2]PF_6$	42.74	2.4	5.61	78.12	11.3	14.46
$[Au(DPQ)Cl_2]PF_6$	42.24	24.7	58.47	71.48	103.8	145.21
$[Au(DPPZ)Cl_2]PF_6$	64.39	29.2	45.35	62.18	128.4	206.50
$[Au(DPQC)Cl_2]PF_6$	45.58	23.3	51.12	60.74	65.9	108.50

IC = Intracellular concentration of gold = $(Au_{ppb}/Protein_{\mu g}) \times 100$.

3.2. Cellular uptake

The cellular uptake of gold complexes was estimated using inductively-coupled plasma (ICP) atomic emission spectroscopy in both cisplatin sensitive and cisplatin resistant cells and the results are represented in Table 2. In A2780 and A2780CP70 cell lines enhanced uptake was observed in $[Au(DPQ)Cl_2]PF_6$ (58.5) and $[Au(DPPZ)Cl_2]PF_6$ (206.5) respectively when compared to other compounds tested. These results indicate that the cellular uptake of gold (III) polypyridyls is cell line dependent. Furthermore, the cytotoxicity parallels the cellular uptake of these compounds suggesting that the intracellular concentrations may be an important factor in dictating cytotoxicity of these compounds. Previous studies have shown that gold complexes undergo cellular uptake via the passive diffusion based on their lipophilicity [31]. However, the lipophilicity of the series of compounds tested was determined to be $[Au(DPQC)Cl_2]PF_6$ > $[Au(DPPZ)Cl_2]PF_6$ > $[Au(DPQ)Cl_2]PF_6$ > $[Au(Phen)Cl_2]PF_6$ which does not correlate with the cellular uptake of these compounds, indicating that the nature of the ligand may influence the cellular uptake through a mechanism other than passive diffusion. Of the four compounds tested, only $[Au(DPQ)Cl_2]PF_6$ and $[Au(DPPZ)Cl_2]PF_6$ exhibited higher cytotoxicity and increased cellular uptake in A2780 and A2780CP70 cells respectively. For this reason, these two compounds were selected for further detailed investigations.

3.3. Reactive oxygen species (ROS) measurement

During our initial studies of gold(III) polypyridyl compounds, we noted significant reactivity in the presence of common biological reducing agents such as reduced glutathione [8]. This reactivity correlates well with the ease of the two electron reduction of gold(III) to gold(I) and thus, may contribute to a mechanism of action that would differ from the more redox stable platinum analog, cisplatin. It followed that the examination of ROS may be a key component in the ability of the gold(III) analogs to overcome resistance to the more redox stable platinum analogs.

The basal ROS was near zero units in A2780CP70 cells, whereas in A2780 cells the ROS was about 40 units (Fig. 4). This observation suggests that the A2780CP70 cell line may also affect its resistance to cisplatin in some ROS diminishing pathway. This being the case, we examined the effect of gold(III) complex addition to measured levels of ROS in both lines. After adding gold(III) polypyridyls, an enhanced ROS production was seen in both cell lines when compared to cisplatin treated cells. The production of ROS in A2780CP70 was lower than A2780 cells. In A2780 and A2780-CP70 cells, AQ and AZ produced greater amounts of ROS respectively.

In the A2780 cell line, addition of $[Au(DPQ)Cl_2]PF_6$ resulted in maximal ROS production whereas $[Au(DPPZ)Cl_2]PF_6$ generated more ROS in the A2780CP70 cells. Treatment of A2780 cells with $[Au(DPQ)Cl_2]PF_6$ resulted in a 420 unit increase in fluorescence intensity and $[Au(DPQ)Cl_2]PF_6$ showed a 380 unit increase compared to cisplatin (Fig. 4). Similarly, both $[Au(DPQ)Cl_2]PF_6$ and $[Au(DPPZ)Cl_2]PF_6$ produced enhanced fluorescence intensity in A2780CP70 cell line by about 25 and 75 units respectively when compared with cisplatin. Redox regulation is critical to cellular function as it influences many signal transduction pathways including the regulation of apoptosis [33]. Cell damage ensues when ROS generation overcomes the cellular antioxidant defenses. Generation of ROS can therefore be exploited therapeutically in the treatment of cancer as the ability of a cell to defend against ROS is associated with resistance to chemotherapy [34]. Previous studies of gold(III) porphyrin complexes have shown that these compounds induce apoptosis by mitochondrial death pathways via the generation of ROS [27]. Taken together, it is possible to speculate that gold polypyridyls may be rendering their cytotoxicity, at least in part, via the generation of ROS.

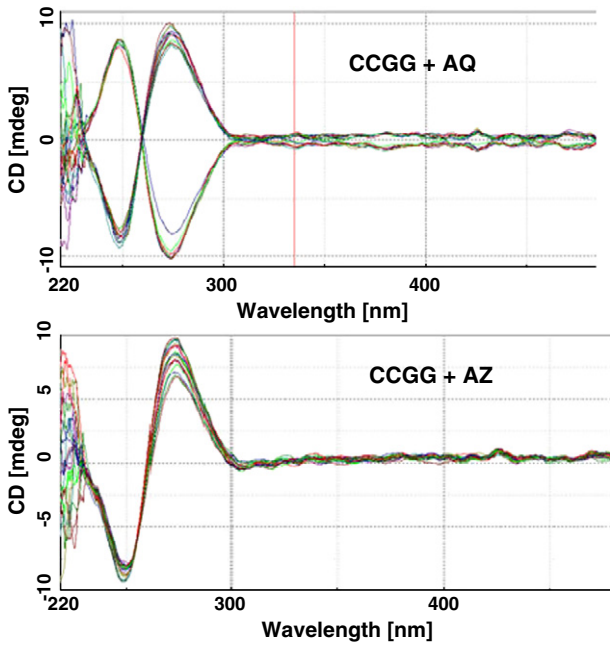

Fig. 5. CD spectrum of synthetic short nucleotide sequences obtained after interaction with gold polypyridyls. CCGG = 5′-CTA TTG CAT AGC CTA TTG CAT AGC-3′5′-GCT ATG CAA TAG GCT ATG CAA TAG-3′. Top: When AQ = $[Au(DPQ)Cl_2]PF_6$ was added to 24mer-DNA, there is a significant change in the shape of the spectrum. This change is primarily due to occupancy of more than one binding site as the compound load on the DNA increases, but may also be due to changes in the DNA conformation. The CD measurements for the $[Au(DPQ)Cl_2]PF_6$ + 24-merDNA exhibits an inversion in absorption maxima at r = 0.09. This change is demonstrative of DNA groove binding. Bottom: The CD intensity changes without a change in the shape of the spectrum as the mole ratio of AZ = $[Au(DPPZ)Cl_2]PF_6$ increases. This change is likely due to intercalative interactions. In general, the different overall shapes of the complexes and the corresponding steric effects imparted by the ligand systems are responsible for the different distortion of DNA structure demonstrated by changes in the corresponding CD spectra.

3.4. CD measurements

To study the interaction of the gold(III) polypyridyls with DNA and the modification of its secondary structure, the CD spectra of calf thymus, plasmid, and synthetic oligonucleotide DNA was obtained in the presence of gold(III) polypyridyls at several molar ratios (r = 0, 0.1, 0.2, 0.3 … 2.0) (Fig. 5). As calf thymus or plasmid DNA failed to produce conclusive results we used short synthetic oligomers (24-mer-GC content 42%) as the primary DNA target. The synthetic oligomer was allowed to interact with gold compounds in physiological buffer, incubated at room temperature for 2 h, and the CD-spectra were measured. Positive bands in the CD spectrum were observed at 273 nm and 216 nm and negative bands were seen at 249 nm and below 200 nm. There is also a conspicuous zero region at 260 nm. A major conformational change occurred when $[Au(DPQ)Cl_2]PF_6$ was added to the synthetic oligomer as indicated by the major reorganization in the CD maxima and minima (Fig. 5). The CD measurements for the $[Au(DPQ)Cl_2]PF_6$ exhibited an inversion in absorption maxima at r = 0.09 indicative of the B → Z transformation. On the other hand, the CD measurements for the $[Au(DPPZ)Cl_2]PF_6$ + DNA exhibited a decrease in absorption intensity which may be explained as an intercalative interaction of this compound with DNA. The aforementioned changes in the CD spectrum suggest that $[Au(DPQ)Cl_2]PF_6$ and $[Au(DPPZ)Cl_2]PF_6$ interacts with DNA through different modes (Fig. 5).

The CD spectra suggest that gold(III) polypyridyls induced modifications in the secondary structure of the DNA double helix and this modification depends on the nature of the polypyridyl ligand. Of note, are the CD spectral differences when the geometry and

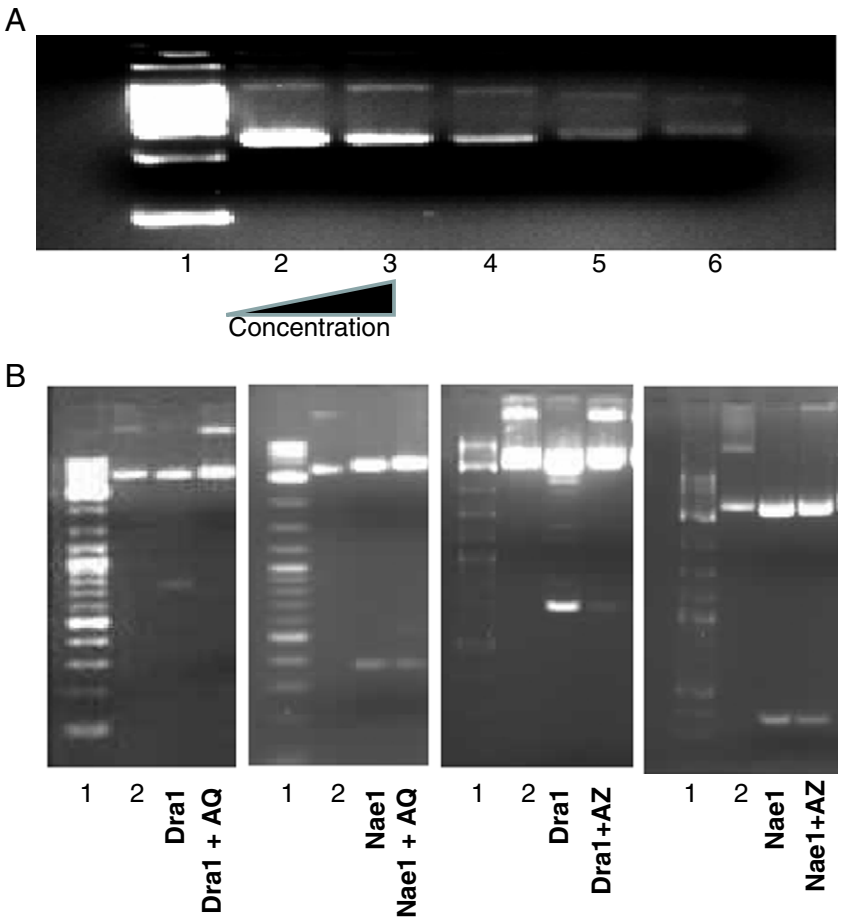

Fig. 6. Restriction enzyme digest of pBR322 plasmid DNA with gold polypyridyls. Panel-A: Interaction of $[Au(DPPZ)Cl_2]PF_6$ (AQ) with pBR322 plasmid. Panel-B: Interaction of $[Au(DPQ)Cl_2]PF_6$ (AQ) and $[Au(DPPZ)Cl_2]PF_6$ (AZ) with pBR322 plasmid and restriction enzymes. 1-Molecular Weight Standard .2-pBR322 Plasmid Dra1-pBR322 Plasmid + Dra1 Restriction Enzyme. Dra1 + AQ/AZ-pBR322 Plasmid + Gold Polypyridyl + Dra1 Restrition Enzyme; Nae1-pBR322 Plasmid + Nae1 Restriction Enzyme. Nae1 + AQ/AZ-pBR322 Plasmid + Gold Polypyridyl + Nae1 Restriction Enzyme.

coordination environment (2N and 2Cl) are similar in both complexes and the only change being the ligands viz., DPQ and DPPZ. Since $[Au(DPQ)Cl_2]PF_6$ presents a more significant change in the CD spectra compared to $[Au(DPPZ)Cl_2]PF_6$, it is possible that the former has a more pronounced effect on DNA structure compared to the latter. The presence or absence of one aromatic ring and the extended aromatic array are key features which may be mediating this interaction. The interaction of the compound with DNA could aid in the retention of the drug within the cells by preventing it from undergoing efflux. This phenomenon may explain the enhanced intracellular retention of these compounds. The different effect on the helical structure DNA, caused by $[Au(DPQ)Cl_2]PF_6$ and $[Au(DPPZ)Cl_2]PF_6$ may also explain the differences in cytotoxicity between these compounds in various cell lines. To better understand whether these compounds are capable of binding to sequence specific sites such as AT and GC rich regions of plasmid DNA, restriction enzyme studies were carried out.

3.5. Interaction of plasmid DNA and gold(III) polypyridyls

Addition of $[Au(DPQ)Cl_2]PF_6$ (AQ) to an equimolar mixture of DNA and ethidium bromide (EB) led to a decrease in fluorescence intensity as shown in Fig. 6 Panel-A. This decrease in fluorescence intensity suggests that gold polypyridyls displace EB from DNA, perhaps by competitive intercalation. Addition of DNA to an incubation mixture of the complexes with EB failed to enhance the fluorescence intensity indicating that EB is unlikely to displace the gold(III) complex from DNA. The DNA gold(III) interaction studies suggests that the binding of EB to pBR322 plasmid is blocked in a stoichiometric manner by the formation of adducts resulting in a loss of fluorescence intensity when the concentration of AQ increases (Fig. 6, Panel-A). As concentration of gold polypyridyl increases, the intensity of linear and cut fragments decreases. Also the shifts in the lengths of the linear and cut fragments as concentration increases are indicative of the plasmid rearrangement. The decrease in intensity has been demonstrated to be mediated by the unwinding of DNA [35]. The decrease in the rate of migration as the concentration of complex increases (Fig. 6 Panel A) can be explained as follows. A compound that unwinds the DNA duplex reduces the number of supercoils in closed circular DNA. This decrease upon binding of the unwinding agent causes attenuation in the rate of migration through agarose gel. This makes it possible to observe and quantify the mean value of unwinding. For closed circular DNA, the topology can be described by linking number 'α' defined by equation "$\alpha = \beta + \tau$", where 'β' is the number of helical turns of the DNA duplex and 'τ' is the numbers of superhelical turns [36]. The linking number remains constant as long as DNA strand breakage does not occur. Compounds that unwind the DNA duplex tend to decrease 'β'. To keep 'α' constant, 'τ', a negative number, must become more positive. The net effect is that the number of supercoils is reduced and the superhelical density of closed circular DNA upon binding of unwinding agents causes a decrease in the rate of migration through agarose. The mobility of the DNA changes gradually and linearly, in proportion to the amount of compound added. A likely explanation is that the binding of the gold compound to DNA does not end up cleaving the DNA but rather may be intercalating the DNA, making it 'bigger' and therefore less mobile. The highest band seems to be running slightly faster in each lane. It is possible

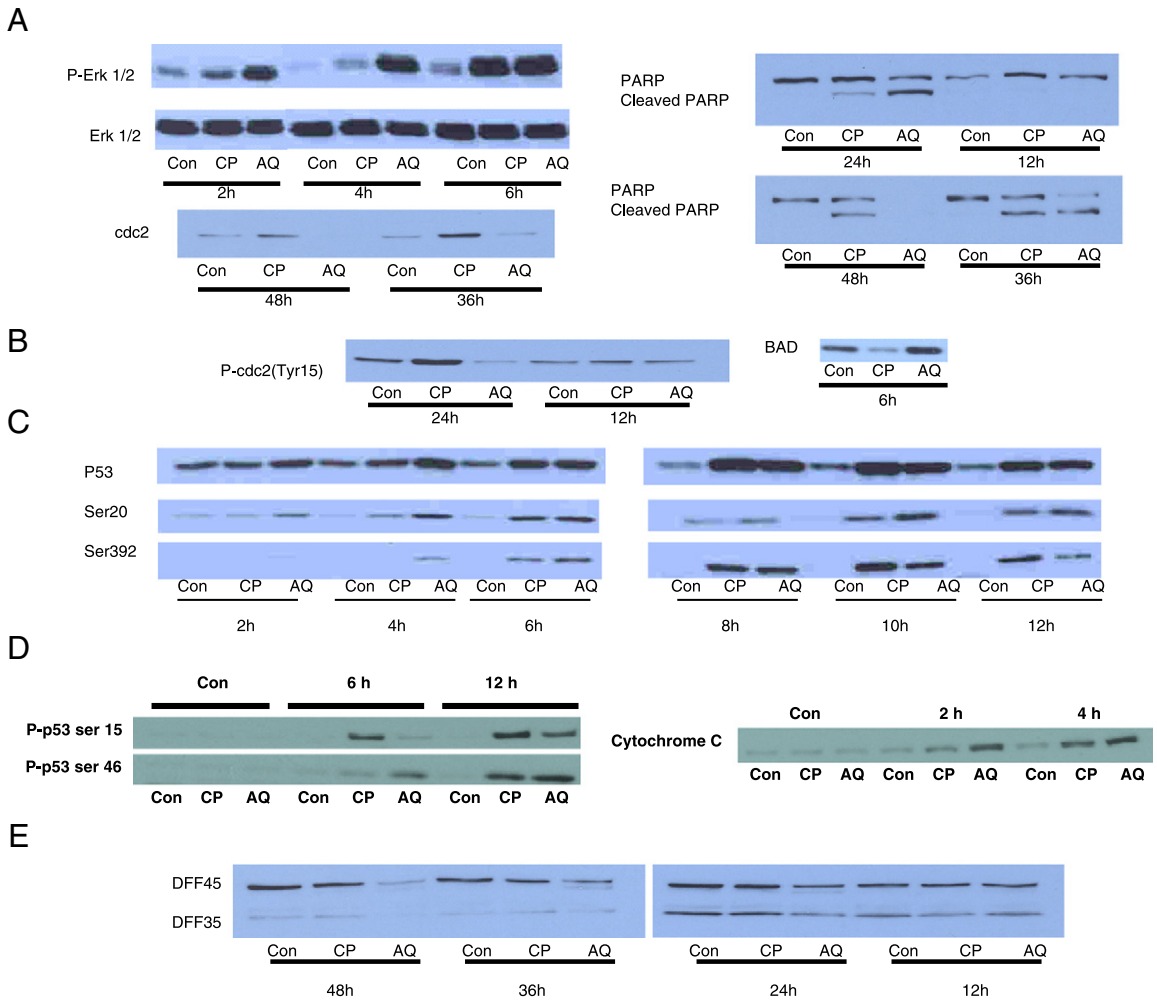

Fig. 7. Intracellular signaling cascades. A2780 cell line was used in this study. Con = Control; CP = Cisplatin; AQ = [Au(DPQ)Cl_2] PF_6. Panel A: P-Erk 1/2, cdc2 and PARP expression levels. Panel B: P-cdc2 and BAD expression levels. Panel C: Experssion levels of p53 and P-p53 after treating the A2780 cells with AQ. Panel D: Expression of P-p53 at residues ser15 and ser46 and cytochrome C. Panel E: Expression levels of DFF45.

the compound is binding and causing it to adopt some secondary structure that is effectively making the DNA less open, and thus running as if it were smaller or more compact. The sharp bands in lanes 2, 3, and 4 exclude the possibility of DNA degradation which is usually appear as a smear. This study supports that gold(III) polypyridyls are capable of interacting with DNA and alter the secondary structure in a detectable manner.

3.6. Restriction enzyme digestion and analysis

With results from CD and plasmid DNA studies suggesting a possible interaction between gold(III) polypyridyls and DNA, we next sought to address the question whether there is a site specific interaction between these compounds and the DNA molecule. Gel electrophoresis following the digestion with *DraI* and *NaeI* of pUC19/pBR322 DNA pre-treated with gold polypyridyls is illustrated in Fig. 6, Panel-B. *DraI* recognizes the sequence "TTTAAA" (TA or AT) and cuts the phosphodiester bond between 3232, 3251 and 3943 bp in pBR322 DNA. *NaeI* recognizes "GCCGGC" (CG or GC) and cuts between 403, 771, 931 and 1285 in pBR322 DNA. The 'AT' sequence was protected from DNase digestion to a greater degree by [Au(DPQ)Cl_2]PF_6, whereas the GC sequence was not. This observation was made based on the fact that *DraI* digestion failed to produce any bands corresponding to the restriction sites. In contrast, [Au(DPPZ)Cl_2]PF_6 failed to protect the restriction sites of either *DraI* and *NaeI* as discerned from the bands appearing in the gel which correspond to the restriction sites of the enzyme. It should also be noted that the concentration of gold polypyridyl complexes used for these experiments were at a 10 fold magnitude lower compared to the concentration of the plasmid DNA as at higher concentrations the bands were masked. Better discrimination between the different gold polypyridyls and restriction endonucleases was achieved with 10 μM concentrations of the test compounds and only these results are presented in Fig. 6, Panel-B. The DNA treated with compounds when digested with restriction enzymes did not show any bands corresponding to the digested product suggesting that the compounds bind to specific DNA sites and protects the sites so that restriction enzymes could not access the site and digest DNA. The compound [Au(DPQ)Cl_2]PF_6 interferes with binding of Dra1 which is AT specific thereby indicating they occupy AT specific sites. Whereas [Au(DPPZ)Cl_2]PF_6 does not interfere with Dra1 or Nae1 indicating that they are neither AT nor GC specific and the possible mode of interaction might be intercalation. This study showed that [Au(DPQ)Cl_2]PF_6 and [Au(DPPZ)Cl_2]PF_6 each interact with DNA through different binding motifs. This finding could provide an additional explanation as to why these compounds are better cytotoxic agents in cisplatin sensitive and resistant cell lines respectively. Should an enhanced DNA repair system contribute to the mechanism of cellular resistance in these or other ovarian cancer cell types, anticancer activity may be altered or enhanced based on whether the agent is specifically an intercalating agent or DNA groove binder. While we are uncertain as to the contribution that enhanced DNA excision repair might play in

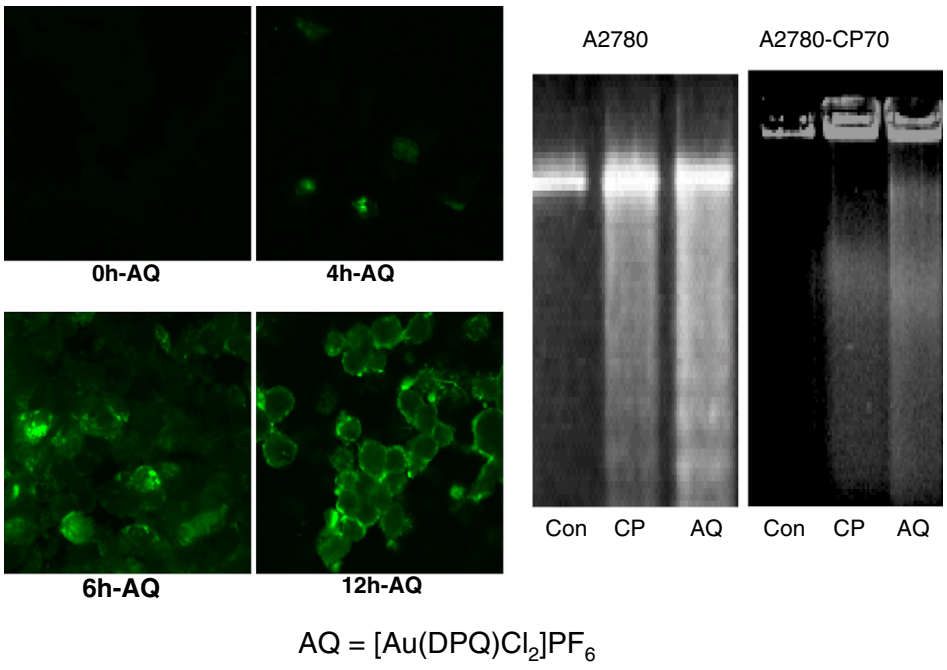

Fig. 8. Apoptotic assay — Annexin V and DNA laddering assay. Con = Cisplatin; AQ = $[Au(DPQ)Cl_2]$ PF_6 and AQ = $[Au(DPQ)Cl_2]PF_6$.

A2780CP70 cells, understanding the nature of the DNA–drug interaction may suggest the role DNA binding type plays in overcoming drug resistance.

Our study is the first restriction enzyme approach for gold polypyridyls to look at the specificity of forming DNA adducts at AT or GC rich regions. Adduct formation by gold polypyridyls with DNA provides a new perspective in the search for better alternatives for platinum chemotherapeutics. Specific and reproducible protection patterns were observed for each DNA interaction study. The protected sequence appears to be the AT binding site and the protected sequences follow the order AT and GC in the case of $[Au(DPQ)Cl_2]PF_6$, whereas $[Au(DPPZ)Cl_2]PF_6$ interaction was primarily through intercalation and to a certain extent AT was more protected than GC. Another possible mechanism of cytotoxicity could be due the inhibition of transcription factors. Transcription factors that perform their function through contacts with specific sequences of DNA, either in the promoter region or distant regions, enhancing or attenuating the initiation of RNA synthesis, are considered as targets of anticancer agents. These contacts may be affected by DNA interacting gold polypyridyls. In a similar study, anthracyclines were assayed on their propensity to inhibit interactions of several transcription factors like Sp1, AP-1, etc. with their recognition sequences [37]. The observations presented in this reference appear consistent with our observations in A2780 and A2780CP70 cell lines.

3.7. Intracellular signaling cascades

Cell death pathways affected by $[Au(DPQ)Cl_2]PF_6$ were evaluated (illustrated in Fig. 7). In general, we observed an overexpression of proapoptotic proteins accompanied by suppression of antiapoptotic proteins following treatment of the cells with gold(III) polypyridyl.

Treatment of cells with the test compound caused a significant upregulation of the mitotic signal Erk 1/2 in a time dependent manner (Fig. 7, Panel-A). SAPK/JNK was elevated at early time points but reached basal levels in 4 h. Erk regulates cell proliferation and drive cell-cycle progression. P38, SAPK(46)/JNK(54) transmit signals in response to cytokines and environmental stress. Activation of both mitogen and stress activated kinase indicates that both the growth factor and cytokine pathways may be affected by $[Au(DPQ)Cl_2]PF_6$. Previous studies have reported that elevated ERK activity contributes to cisplatin- induced cell death [38]. Erk works upstream of caspases such that inhibition of ERK activity inhibits apoptosis. This appears to play an active role in mediating cisplatin-induced apoptosis [36]. Activation of MAPK pathway by ROS has been well known [39–41]. Whereas transient activation of MAPK triggers cell proliferation, prolonged or sustained activation of MAPK leads to cell death [42]. The ROS generated by gold(III) polypyridyls may be mediating cell death through the activation of proapoptotic signals [41].

$[Au(DPQ)Cl_2]PF_6$ arrests cell cycle machinery at the mitotic (M) phase by attenuating cdc2 kinase (Fig. 7, Panel-A). Entry of cells into the M phase of the cell cycle is regulated by activation of cdc2 kinase. The critical regulatory step in activating cdc2 during progression into mitosis appears to be the dephosphorylation of tyrosine 15. $[Au(DPQ)Cl_2]PF_6$ dephosphorylates cdc2 at Tyr15 (Fig. 7, Panel-B). In A2780CP70 cell lines, mismatch repair (MMR) is a highly conserved repair system that correlates mismatches arising during DNA replication and safeguards genomic integrity [43]. MMR participates in the regulation of the G2-M cell cycle check point and a G2 arrest by signaling the cdc2 pathway [43]. Inhibitory phosphorylation of cdc2 is essential for the p53 independent G2 arrest that occurs in response to DNA damage [44].

While p53 plays a major role in cellular response to DNA damage and other genomic aberrations [45], activation of p53 can lead to cell cycle arrest and/or DNA repair or apoptosis [46]. Expression levels of p53 in A2780 (Fig. 7, Panel-C) and A2780CP70 were increased following treatment with gold(III) polypyridyls. Furthermore, treatment of $[Au(DPQ)Cl_2]PF_6$ induced phosphorylation of p53 at Ser 15 and Ser 20 residues (Fig. 7, Panels-C and -D). After 4 h treatment with $[Au(DPQ)Cl_2]PF_6$, phosphorylation of p53 at Ser 392 was more pronounced than that observed with cisplatin. Phosphorylation at Ser 392 promotes the growth suppressor function, DNA binding, and transcriptional activation of p53. Treatment of cells with gold polypyridyls also caused an upregulation of the phosphorylation at Se r46 residue on p53 (Fig. 7, Panel-D). This site has been recognized to be important for regulating the ability of p53 to induce apoptosis [47]. Cisplatin resistant cells exhibited decreased platinum accumulation, reduced levels of platinum bound DNA and increased tolerance to drug induced DNA damage and decreased DNA repair. Forced

induction of p53 has been shown to cause a 10-fold increase in sensitivity of cancer cells to cisplatin induced cytotoxicity [48]. Cell cycle arrest mediated by p53 allows the host cell to repair its damaged DNA before cell division while cells with excessive DNA damage undergo apoptosis. It has been demonstrated that decreased apoptosis in A2780CP70 cells compared to the parental A2780 cells is due to the decreased p53 induction in A2780CP70 cell line. Even though both the cell lines had equivalent levels of DNA damage, resistance in this model system correlated with attenuation of p53 induction and decreased apoptotic stimuli rather than with differences in cell cycle response [49]. The higher levels of p53 in response to gold(III) polypyridyls compared to cisplatin further supports the use of these gold(III) compounds as an alternative to overcome cisplatin resistance.

It has been shown that cells sensitive to p53 mediated apoptosis produce ROS concomitantly with p53 over expression, whereas cells resistant to p53 failed to produce ROS. In sensitive cells, both ROS production and apoptosis were inhibited by antioxidant treatment [50]. In addition to generation of ROS, apoptosis in A2780 and A2780CP70 is associated with increased levels of BAK and BAX after drug-induced damage and that functional p53 may be required to execute apoptotic effect [51]. It has also been reported that gold(III) porphyrin binds DNA through non-covalent interaction [48]. Gold (III) porphyrin enhances p53 expression to arrest cell cycle at G0–G1, and induces apoptosis [52]. All of these findings provide precedent for our assertions in the action of gold(III) polypyridyl complex activity.

The increase in pro-death signals such as cleaved PARP, DFF 45/35, etc. which are targets of caspases, all lead to increased apoptotic stimulus. Further, we observed the activation of proapoptotic BAD (Fig. 7, Panel-B). Dephosphorylation of BAD indicates the abrogation of the pro-survival Akt pathway. It has been reported that gold(III) dithiocarbamate derivatives suppressed tumor cell growth in a dose-dependent manner [44]. The gold(III) compounds, but not cisplatin, were able to down regulate the antiapoptotic molecule Bcl-2, up regulate the proapoptotic molecule BAX and induce apoptosis. These findings suggest that gold(III) compounds induce apoptosis via BAX/BAD pathway.

Poly (ADP-ribose) polymerase (PARP), a DNA repair enzyme activated by genotoxic stress, is essential for the proper recruitment of base excision repair (BER) components to the N^3-methyladenine and N^7-methylguanine adducts formed as a result of DNA alkylation. The activation of downstream caspase-3 by most agents leads to the cleavage of the PARP protein [53]. Cleavage of PARP results in loss of BER capacity, mediating the apoptotic pathway through downstream effector caspases. The cells treated with gold(III) polypyridyls activated PARP cleavage (Fig. 7, Panel-A) in a time-dependent manner and the cleaved PARP levels were higher than that seen in cisplatin treated cells. Increased expression of cleaved PARP suggests that gold(III) polypyridyls are better drugs for mismatch repair (MMR)-deficient and proficient cell lines, and would result in cytotoxicity independent of cisplatin resistance.

The increase in cytochrome C release (Fig. 7, Panel-D) and inhibition of DNA fragmentation factor (DFF) signals (Fig. 7, Panel-E) after treating the cells with gold(III) polypyridyls shows that these compounds mediate cell death through apoptosis. Caspase-3 is believed to be the primary enzyme responsible for processing DFF45. The association of DNA fragmentation factor (DFF)-45 (or its isoform DFF35) with DFF40 inhibits the DNAse activity. The cleavage of DFF45 inactivates its inhibitory function on DFF40 and causes nuclear DNA degradation by DFF40 leading to cell death. Gold(III) polypyridyl inhibits DNAse activity (Fig. 7, Panel-E), the association of DFF45 (or its isoform DFF35) with DFF40 inhibits the DNAse activity. DFF45 has been shown to be the target of caspase-3, -6, -7, -8 and granzyme B. Taken together, it is evident that gold(III) polyprydidyls cause an elevation in the intracellular pro-apoptotic signals while blunting the antiapoptotic signals.

The confocal image of cells after treatment with compounds is shown in (Fig. 8). Initiation of apoptosis occurs at 2 h and continued over a period of 10 h. Maximal apoptotic cells were observed at 12 h after addition of AQ to cells. The onset of apoptosis occurs after 4 h and continues until 12 h showing peak apoptosis. DNA laddering was used as an additional method to assess the effect of the complexes on apoptosis (Fig. 8). Even though laddering smear pattern of DNA was seen in the DNA of cells after treating them with CP and AQ, the laddering and smear was significantly more prominent in AQ treated cells. Apoptosis is associated with the fragmentation of chromosomal DNA into multiples of the 180 bp nucleosomal unit and due to this fragmentation, the DNA shows a laddering pattern when electrophoresed. As seen in Fig. 8 for the same amount of DNA the laddering effect was more pronounced in gold(III) polypyridyl treated cell lines than the one treated with cisplatin.

4. Summary and conclusion

Through this study we demonstrated that gold(III) polypyridyls can and do overcome cisplatin resistance and that their cytotoxicity can be modified by varying the ligand environment. At the molecular level, these compounds demonstrate improved cellular uptake and DNA binding compared to cisplatin. The ligand geometry of gold(III) polypyridyls appear to alter the DNA binding modes. Further, this study suggests that gold(III) polypyridyls are viable alternatives to cisplatin and their anticancer activity and selectivity may be fine tuned by polypyridyl structural variation. Mechanistically, gold(III) polypyridyls are believed to activate cell death machinery through an increased ROS production. In the normal non-cancer cells the cytotoxicity of gold(III) polypyridyls was lower than that of cisplatin. The intracellular signaling cascades shows that $[Au(DPQ)Cl_2]PF_6$ upregulates tumor suppressor p53 and activates other anti-survival pathways leading to cell cycle arrest and induction of apoptosis.

References

[1] T.S.L. Vincent, T. Devita, S.A. Rosenberg, Cancer: Principles and Practice of Oncology, Lippincott Williams and Wilkins, 2008, pp. 419–426.
[2] A.K. Godwin, A. Meister, P.J. O'Dwyer, C.S. Huang, T.C. Hamilton, M.E. Anderson, Proceedings of the National Academy of Sciences of the United States of America 89 (1992) 3070–3074.
[3] Z.H. Siddik, Oncogene 22 (2003) 7265–7279.
[4] A. Casini, C. Hartinger, C. Gabbiani, E. Mini, P.J. Dyson, B.K. Keppler, L. Messori, Journal of Inorganic Biochemistry 102 (2008) 564–575.
[5] L. Messori, F. Abbate, G. Marcon, P. Orioli, M. Fontani, E. Mini, T. Mazzei, S. Carotti, T. O'Connell, P. Zanello, Journal of Medicinal Chemistry 43 (2000) 3541–3548.
[6] V. Milacic, D. Chen, L. Ronconi, K.R. Landis-Piwowar, D. Fregona, Q.P. Dou, Cancer Research 66 (2006) 10478–10486.
[7] L. Ronconi, C. Marzano, P. Zanello, M. Corsini, G. Miolo, C. Macca, A. Trevisan, D. Fregona, Journal of Medicinal Chemistry 49 (2006) 1648–1657.
[8] K. Palanichamy, A.C. Ontko, Inorganica Chimica Acta 359 (2006) 44–52.
[9] P. Shi, Q. Jiang, Y. Zhao, Y. Zhang, J. Lin, L. Lin, J. Ding, Z. Guo, Journal of Biological Inorganic Chemistry 11 (2006) 745–752.
[10] B.M. Zeglis, J.K. Barton, Nature Protocols 2 (2007) 357–371.
[11] B.M. Zeglis, J.A. Boland, J.K. Barton, Biochemistry 48 (2009) 839–849.
[12] B.M. Zeglis, V.C. Pierre, J.T. Kaiser, J.K. Barton, Biochemistry 48 (2009) 4247–4253.
[13] C.A. Puckett, J.K. Barton, Biochemistry 47 (2008) 11711–11716.
[14] P.K. Bhattacharya, J. Cha, J.K. Barton, Nucleic Acids Research 30 (2002) 4740–4750.
[15] E.M. Boon, J.L. Kisko, J.K. Barton, Redox Cell Biology and Genetics Part B 353 (2002) 506–522.
[16] L.N. Ji, Q.L. Zhang, H. Chao, Chinese Science Bulletin 46 (2001) 1332–1337.
[17] E.R. Tiekink, Inflammopharmacology 16 (2008) 138–142.
[18] G. Marcon, S. Carotti, M. Coronnello, L. Messori, E. Mini, P. Orioli, T. Mazzei, M.A. Cinellu, G. Minghetti, Journal of Medicinal Chemistry 45 (2002) 1672–1677.
[19] G. Marcon, L. Messori, P. Orioli, Expert Review of Anticancer Therapy 2 (2002) 337–346.
[20] A. Bindoli, M.P. Rigobello, G. Scutari, C. Gabbiani, A. Casini, L. Messori, Coordination Chemistry Reviews 253 (2009) 1692–1707.
[21] F. Magherini, A. Modesti, L. Bini, M. Puglia, I. Landini, S. Nobili, E. Mini, M.A. Cinellu, C. Gabbiani, L. Messori, Journal of Biological Inorganic Chemistry 15 (2010) 573–582.
[22] K.H. Chow, R.W. Sun, J.B. Lam, C.K. Li, A. Xu, D.L. Ma, R. Abagyan, Y. Wang, C.M. Che, Cancer Research 70 (2010) 329–337.

[23] J.J. Yan, A.L.F. Chow, C.H. Leung, R.W.Y. Sun, D.L. Ma, C.M. Che, Chemical Communications 46 (2010) 3893–3895.
[24] C.F. Shaw, Chemical Reviews 99 (1999) 2589–2600.
[25] C.M. Che, R.W.Y. Sun, W.Y. Yu, C.B. Ko, N.Y. Zhu, H.Z. Sun, Chemical Communications (2003) 1718–1719.
[26] X. Meng, W. Cai, D.C. Schwartz, Journal of Biomolecular Structure and Dynamics 13 (1996) 945–951.
[27] A.M. Rogan, T.C. Hamilton, R.C. Young, R.W. Klecker Jr., R.F. Ozols, Science 224 (1984) 994–996.
[28] J.A. Green, D.T. Vistica, R.C. Young, T.C. Hamilton, A.M. Rogan, R.F. Ozols, Cancer Research 44 (1984) 5427–5431.
[29] R.W. Sun, C.K. Li, D.L. Ma, J.J. Yan, C.N. Lok, C.H. Leung, N. Zhu, C.M. Che, Chemistry A European Journal 16 (2010) 3097–3113.
[30] M. Kartalou, J.M. Essigmann, Mutation Research 478 (2001) 23–43.
[31] D.P. Gately, S.B. Howell, British Journal of Cancer 67 (1993) 1171–1176.
[32] X.L. Ren Lirong, J. Hu, Z. Li, Z. Wang, Journal of Huazhong University of Science and Technology 27 (2007) 721–724.
[33] P. Costantini, E. Jacotot, D. Decaudin, G. Kroemer, Journal of the National Cancer Institute 92 (2000) 1042–1053.
[34] M.F. Renschler, European Journal of Cancer 40 (2004) 1934–1940.
[35] M.V. Keck, S.J. Lippard, Journal of the American Chemical Society 114 (1992) 3386–3390.
[36] W.R. Bauer, Annual Review of Biophysics & Bioengineering 7 (1978) 287–313.
[37] A. Szulawska, M. Gniazdowski, M. Czyz, Biochemistry and Pharmacology 69 (2005) 7–18.
[38] X. Wang, J.L. Martindale, N.J. Holbrook, Journal of Biological Chemistry 275 (2000) 39435–39443.
[39] J.L. Martindale, N.J. Holbrook, Journal of Cellular Physiology 192 (2002) 1–15.
[40] B.G. Park, C.I. Yoo, H.T. Kim, C.H. Kwon, Y.K. Kim, Toxicology 215 (2005) 115–125.
[41] M.R. Kim, H.S. Chang, B.H. Kim, S. Kim, S.H. Baek, J.H. Kim, S.R. Lee, J.R. Kim, Biochemical and Biophysical Research Communications 304 (2003) 119–124.
[42] S. Sakon, X. Xue, M. Takekawa, T. Sasazuki, T. Okazaki, Y. Kojima, J.H. Piao, H. Yagita, K. Okumura, T. Doi, H. Nakano, EMBO Journal 22 (2003) 3898–3909.
[43] T. Yan, J.E. Schupp, H.S. Hwang, M.W. Wagner, S.E. Berry, S. Strickfaden, M.L. Veigl, W.D. Sedwick, D.A. Boothman, T.J. Kinsella, Cancer Research 61 (2001) 8290–8297.
[44] C. Norbury, J. Blow, P. Nurse, EMBO Journal 10 (1991) 3321–3329.
[45] D.W. Meek, C.W. Anderson, Cold Spring Harbor Perspectives in Biology 1 (2009) a000950.
[46] A.J. Levine, Cell 88 (1997) 323–331.
[47] K. Oda, H. Arakawa, T. Tanaka, K. Matsuda, C. Tanikawa, T. Mori, H. Nishimori, K. Tamai, T. Tokino, Y. Nakamura, Y. Taya, Cell 102 (2000) 849–862.
[48] J. Fan, J.R. Bertino, Molecular Pharmacology 56 (1999) 966–972.
[49] A. Vaisman, M. Varchenko, I. Said, S.G. Chaney, Cytometry 27 (1997) 54–64.
[50] T.M. Johnson, Z.X. Yu, V.J. Ferrans, R.A. Lowenstein, T. Finkel, Proceedings of the National Academy of Sciences of the United States of America 93 (1996) 11848–11852.
[51] N.A. Jones, J. Turner, A.J. McIlwrath, R. Brown, C. Dive, Molecular Pharmacology 53 (1998) 819–826.
[52] Y. Wang, Q.Y. He, R.W. Sun, C.M. Che, J.F. Chiu, European Journal of Pharmacology 554 (2007) 113–122.
[53] M. Tewari, L.T. Quan, K. O'Rourke, S. Desnoyers, Z. Zeng, D.R. Beidler, G.G. Poirier, G.S. Salvesen, V.M. Dixit, Cell 81 (1995) 801–809.